ELSEVIER

Biophysical Chemistry 67 (1997) 107–116

Biophysical Chemistry

Salt and pH effects on electrochemistry of myoglobin in thick films of a bilayer-forming surfactant

Alaa-Eldin F. Nassar [a,1], James F. Rusling [a,*], Thomas F. Kumosinski [b]

[a] *Department of Chemistry, Box U-60, University of Connecticut, Storrs, CT 06269-4060, USA*
[b] *Eastern Regional Research Center, US Department of Agriculture, Wydmoor, PA 19038-8551, USA*

Received 18 December 1996; revised 3 February 1997; accepted 3 February 1997

Abstract

Salt concentration and pH of external solutions were shown to control the electrochemistry of the heme protein myoglobin (MbFe(III)–H_2O) in stable, ordered films of didodecyldimethylammonium bromide (DDAB). Protonation of aquometmyoglobin (MbFe(III)–H_2O) in these films precedes electron transfer from electrodes, causing formal potentials to shift negative as pH increases from 5 to 8. At pH > 8, MbFe(III)–H_2O dissociates to MbFe(III)–OH, which is reduced directly at the electrode at higher rates than MbFe(III)–H_2O. Correlations of voltammetric data with FT–IR spectra suggested that at pH < 4.6, an unfolded form of Mb resides in the films and is reduced directly. The concentration of salt in solution influences electrochemical properties of Mb-DDAB films by its influence on Mb conformation and by effects on interfacial Donnan potentials. NMR indicated strong binding of anions to Mb within DDAB films. Bound anions may neutralize positive charge on Mb's surface so that it can reside in a partly hydrophobic environment, as postulated on the basis of previous ESR and linear dichroism studies. © 1997 Elsevier Science B.V.

Keywords: Myoglobin; Electron transfer; Protein-surfactant films; Salt effects; Protein unfolding

1. Introduction

Electrochemical studies of protein redox reactions in biomembrane-like environments may be useful for elucidating chemistry related to biological function and disease states. However, achieving direct electron transfer between electrodes and proteins in solution may encounter major difficulties. Adsorption of macromolecular impurities or the protein itself on the electrode may block electron transfer [1,2]. Impressive progress in electrode coatings which facilitate protein electron transfer has been made recently [1–4], with several examples mimicking biomembranes [4–16].

We recently reported [17] reversible electron transfer between electrodes and the iron heme protein myoglobin (Mb) imbedded in stable, lamellar liquid crystal films of didodecyldimethylammonium bromide (DDAB). Rates of electron transfer involving Mb heme Fe(III)/Fe(II) were much faster than for myoglobin in solution using bare electrodes [18–20]. We have since used a variety of water insoluble surfactants, including phosphatidylcholines, to make stable films of myoglobin with reversible electron transfer properties on metal and carbon electrodes [21–23]. These films have structures which feature

* Corresponding author.
[1] Present address: Battelle Institute, 2012 Tollgate Rd., Bel Air, MD 21015, USA.

PII S0301-4622(97)00027-6

lipid-bilayer-like multilayers. Myoglobin is specifically oriented within them [17,21–24], and is likely to be partly associated with hydrophobic regions of the bilayers [24]. Such films have also provided good electron transfer for other proteins and enzymes including cytochrome $P450_{cam}$ [25], hemoglobin [26], c-type cytochromes [27–29], and ferredoxins [30–32].

While studies of proteins in surfactant films have addressed electron transfer properties [17,21–32], catalytic reactions with small molecules [33], and static supramolecular structures [24], specific features which contribute to protein-surfactant film properties are somewhat uncertain. Recent studies on thin films of phosphatidyl cholines or DDAB containing Mb showed that the pH of the external solution controls protein conformation and influences redox properties [34]. However, questions remain about how external solution properties, including salt concentration, influence electron transfer properties of the protein and its secondary structure within the film.

In this paper, we report the influence of salt concentration and pH of the external solution on the properties of 20 μm thick films of DDAB containing myoglobin. Results suggest that salt and pH influence these films by their effect on protein secondary structure, heme iron ligation state, and interfacial Donnan potentials.

2. Experimental

2.1. Materials and solutions

Horse myoglobin (Sigma) in buffer was passed through Amicon YM30 filters (30000 MW cutoff) [23]. Concentrations after filtration were estimated by visible spectroscopy [17]. Didodecyldimethylammonium bromide (DDAB, 99 + %) was from Kodak. Sodium acetate-d_3 ($C_2D_3O_2Na$) and acetic-d_3 acid-d ($C_2D_4O_2$) were from Sigma. All other chemicals were reagent grade.

Buffers included 10 mM acetate + 50 mM NaBr, pH 4–6, 10 mM *tris*-hydroxymethylaminomethane · HCl + 50 mM NaCl or NaBr, pH 6.5–9.0. Water was purified with a Barnstead–Nanopure system to specific resistance > 15 MΩ cm.

2.2. Apparatus and procedures

Methods and apparatus for cyclic voltammetry (CV) were described previously [17,21–23]. Oxygen was removed by purging solutions with purified nitrogen. Films were cast onto basal plane ordinary pyrolytic graphite (PG) disks (HPG-99, Union Carbide; geometric $A = 0.2$ cm^2) previously abraded on 600-grit SiC paper. Potentials are referred to the saturated calomel reference electrode (SCE). Ohmic drop was fully compensated. All experiments were done at 25°C.

Films were cast onto PG electrodes from clear vesicle dispersions of 5 mM DDAB after adding Mb to 0.25 mM. 10 μl of this mixture was spread evenly onto an electrode and dried overnight to give films about 20 μm thick, as described previously [24].

CVs of films were done in buffers containing no Mb. Apparent standard heterogeneous electron transfer rate constants ($k^{0'}$) for Mb were obtained from diffusion controlled CVs as described previously [17,21,23].

Films were cast onto aluminum-coated glass for reflectance-absorbance FT–IR, as described previously [17]. Deuterium and ^{35}Cl-NMR were done by using a Bruker AC-270 spectrometer. Standards were cesium chloride for ^{35}Cl, and CD_3COOH for ^{2}D. DDAB films on PG were soaked overnight in buffers, washed with water, scrapped off the PG into NMR tubes, and dispersed with chloroform or ethanol for NMR analyses.

3. Results

3.1. Influence of pH on voltammetry

Cyclic voltammetry (CV) of myoglobin (Mb) showed a strong dependence on pH in thick DDAB films. The nearly reversible heme Fe(III)/Fe(II) peaks in Fig. 1 shift to more negative potentials and change shape with increasing pH. Peak current at pH 9 is significantly smaller than at pH 4. All changes with pH were reversible. That is, CVs of a given film were identical to those in Fig. 1 upon switching between any two buffers in the range pH 4–9.

Shapes of CVs at scan rate (ν) > 50 mV s^{-1} were diffusion controlled (Fig. 1), as reported previ-

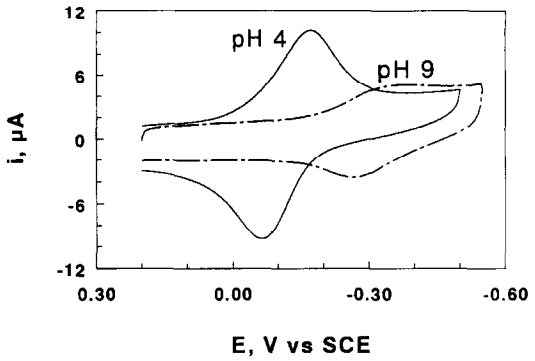

Fig. 1. Cyclic voltammograms of Mb-DDAB film on PG electrode in buffers of pH 4.0 and 9.0 containing 50 mM NaBr at 0.1 V s^{-1}.

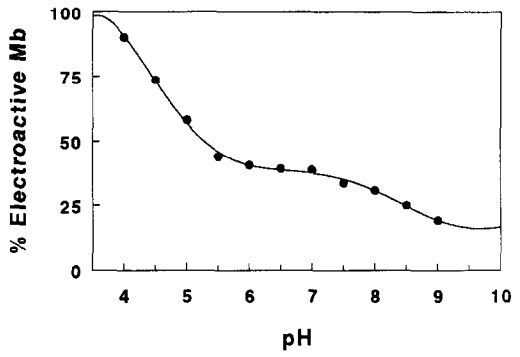

Fig. 3. Influence of pH on percent of electroactive Mb in DDAB films in 10 mM buffers containing 50 mM NaBr or NaCl. The total amount of Mb in the films was 2.5 nmol. Solid line represents best fit by nonlinear regression onto the model in Eq. (3).

ously [17,23]. At $\nu < 6$ mV s^{-1}, thin layer electrochemical behavior was observed, in which all electroactive MbFe(III) in the films is converted to MbFe(II) on the cathodic scan.

Formal potentials ($E^{0'}$) of the Mb heme Fe(III)/Fe(II) couple in DDAB films were estimated as midpoints between anodic and cathodic peak potentials. Plots of $E^{0'}$ vs. pH had linear regions between pH 5 and 8 (Fig. 2), with a slope of 65 ± 3 mV/pH unit. This is consistent with the transfer of one proton and one electron during reduction [35,36] of MbFe(III).

$E^{0'}$-values were roughly independent of pH between pH 4 and 4.8 (Fig. 2). Their pH dependencies resemble that for the electrochemical reduction of a weak acid [35,36]. The intersection point at pH 4.8 suggests reduction of a protonated form of the protein with $pK_a = 4.8$.

Integrations of thin-layer CVs at $\nu < 6$ mV s^{-1} provided the number of moles of electroactive protein in the films. Dividing by the known amount of protein deposited on the electrode gave the percent of electroactive protein in the films. In Mb-DDAB films, this quantity varied with pH (Fig. 3), reaching nearly 100% at low pH, dropping to 40% in the medium pH range, and approaching 20% at pH 9.

Apparent standard heterogeneous electron transfer rate constants ($k^{0'}$) also varied systematically with pH (Fig. 4). These $k^{0'}$ values are rate constants at $E^{0'}$. Values show a small decrease from pH 4–5.5, and a large increase as pH increased from 7 to 9.

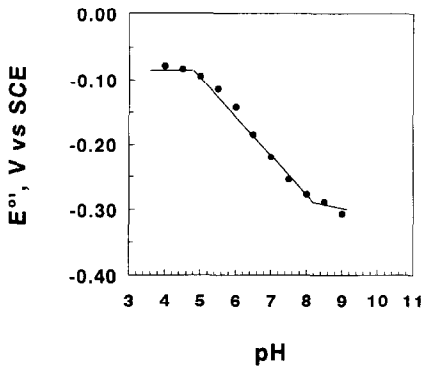

Fig. 2. Influence of pH on formal potential of Mb in DDAB films in 10 mM buffers containing 50 mM NaBr or NaCl.

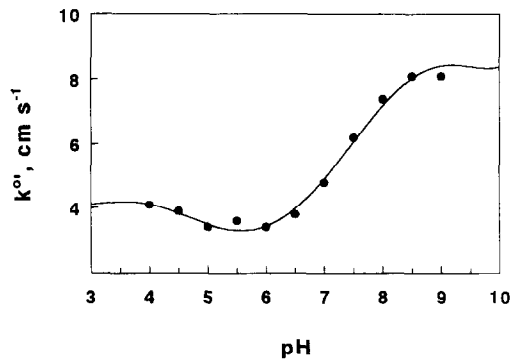

Fig. 4. Influence of pH on apparent standard heterogeneous rate constant ($k^{0'}$) for film of Mb-DDAB in 10 mM buffers containing 50 mM NaBr or NaCl. Solid line represents best fit by nonlinear regression onto the model in Eq. (3).

3.2. Influence of salt on voltammetry

Since myoglobin conformation is influenced by salt concentration in solution, [37,38] we measured electrochemical parameters of the films over a range of salt and buffer concentrations. Percent electroactive Mb in DDAB films at pH 7.5 showed almost no dependence on salt (Fig. 5) or buffer concentration (+50 mM NaBr) in the external solution. At pH 5.5, percent electroactive Mb increased slightly with increasing [NaBr], and showed a small maximum at 70 mM salt. At pH 4, a maximum of nearly 90% electroactive Mb was found at 50 mM NaBr, with a decrease to 36% at 75 mM NaBr. There was also a slight dependence of percent electroactive Mb on buffer concentration in 50 mM NaBr solutions.

$E^{0'}$ and $k^{0'}$-values for Mb in DDAB films increased linearly when plotted against the log of salt or buffer concentration, as illustrated by dependences on [NaBr] (Figs. 6 and 7). Slopes of plots of $E^{0'}$ vs. log[NaBr] were similar at pH 4 and 7.5, and slightly larger at pH 5.5 (Table 1). Slopes of similar plots vs. log[buffer] with 50 mM NaBr present were about half of those in Fig. 6. Slopes of plots of $k^{0'}$ vs. log[NaBr] or log[buffer] were similar at pH 5.5 and 7.5, but [NaBr] had a much smaller influence on $k^{0'}$ at pH 4 (Fig. 7 and Table 1).

In a previous study, films were prepared by soaking DDAB films in Mb solutions containing acetate or chloride ions [17]. These films had nearly identical electrochemical properties to those discussed here. Energy dispersive X-ray (EDX) analysis of these Mb-DDAB films gave a Br/C ratio 3-fold smaller than for DDAB films soaked in the same buffer solution without Mb. These EDX results suggested that bromide ions were replaced in the DDAB films by anions from solution only in the presence of protein. The decrease in amount of bromide in the films in the presence of Mb can not be explained by interactions of surfactant with Mb surface charges, which are positive at pH < 7. We speculated that Mb might bring bound anions into the film [17].

In the present work, we used ^{35}Cl- and D-NMR to investigate anion binding to Mb in buffers containing chloride or deuterated acetate. Buffers were 10 mM TRIS + 50 mM NaCl, pH 7.5, and 10 mM deuterated acetate + 50 mM NaBr, pH 5.5. NMR spectra were the same whether films were prepared from Mb-surfactant vesicle dispersions, as in the rest of this paper, or by soaking separately prepared DDAB films in Mb solutions. Significant Cl^- was detected in DDAB films soaked in the Mb-containing TRIS–NaCl buffer (Fig. 8) as well as in films prepared

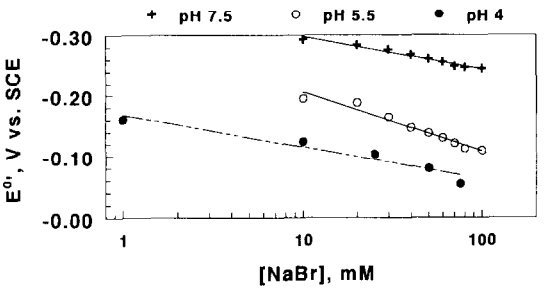

Fig. 6. Influence of concentration of sodium bromide on formal potentials of Mb-DDAB films in 10 mM buffers with different pH values. Lines obtained by linear regression.

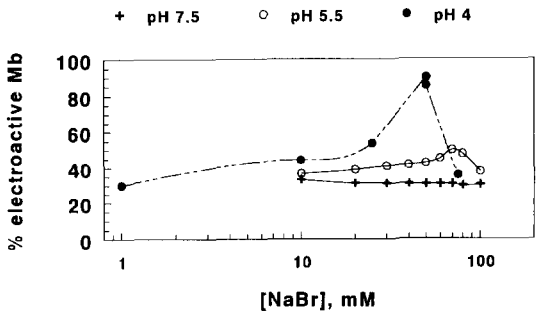

Fig. 5. Influence of concentration of sodium bromide on percent of electroactive myoglobin in DDAB films in 10 mM buffers with different pH values.

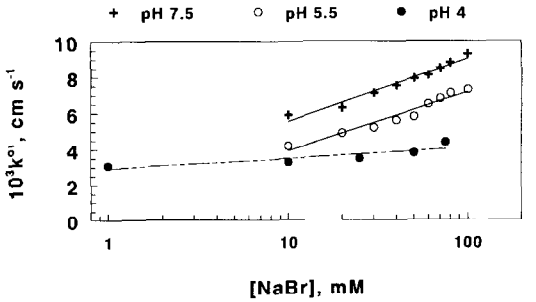

Fig. 7. Influence of concentration of sodium bromide on apparent standard heterogeneous rate constant of Mb in DDAB films in 10 mM buffers with different pH values. Lines were obtained by linear regression.

Table 1
Influence of salt and buffer concentration on formal potentials and electron transfer rate constants of Mb in DDAB films

Variable (S)	$dE^{0'}/d\log[S]$ (V $\log[S]^{-1}$)	$dk^{0'}/d\log[S]$ (cm s^{-1} $\log[S]^{-1}$)
[NaBr] in pH 4 acetate buffer	53	0.6×10^{-3}
[Acetate] at pH 5.5 + 50 mM NaBr	32	2.7×10^{-3}
[NaBr] in pH 5.5 acetate buffer	97	3.2×10^{-3}
[TRIS] at pH 7.5 + 50 mM NaBr	27	2.8×10^{-3}
[NaBr] at pH 7.5 TRIS buffer	53	3.5×10^{-3}

from Mb-vesicle dispersions in this buffer. DDAB films soaked in protein-free buffer gave no ^{35}Cl signals.

For films prepared with deuterated acetate buffer, only films containing Mb showed characteristic CD_3-NMR peaks for deuterated acetate. Thus, NMR spectra suggest selective binding of Cl^- and acetate to Mb within the films. Bromide may also bind to Mb, but we have no probe to detect it. In any case, Cl^- and acetate seem to compete well with Br^- for adsorption sites on the protein.

3.3. Reflectance-absorbance FT–IR spectra

The amide I band (1700–1600 cm^{-1}) of proteins is caused by C=O stretching of peptide linkages. Its shape is sensitive to secondary structure. Amide bands of proteins consist of many overlapped components, reflecting the various environments of carbonyl groups in the protein [39–42]. Absorbance from DDAB does not occur in the amide I region.

It was reported that reflectance-absorbance infrared (RAIR) spectra of Mb-surfactant films were similar to spectra of films of Mb alone between pH 5.5 and 7.5 [17] where the protein has its native conformation in solution. The present study confirms that finding, but careful inspection of second derivative RAIR spectra revealed subtle differences which depend on pH. Similar changes in spectra with pH were found at source incidence angles of 45°, 60° and 75°.

The second derivative of any symmetric peak has a negative peak at the position of the original maximum between two smaller positive peaks. Thus, the strong negative peak at about 1660 cm^{-1} in spectra of the pure Mb film without surfactant (Fig. 9) is characteristic of a major component of the amide I band. This 1660 cm^{-1} band is assigned [40–42] to α-helix. At pH 4, this peak becomes smaller and is accompanied by a new band close to 1630 cm^{-1} [34], assigned to extended disordered features of the polypeptide backbone. The spectra in films without surfactant are similar to those in solution.

The main feature in the second derivative amide I

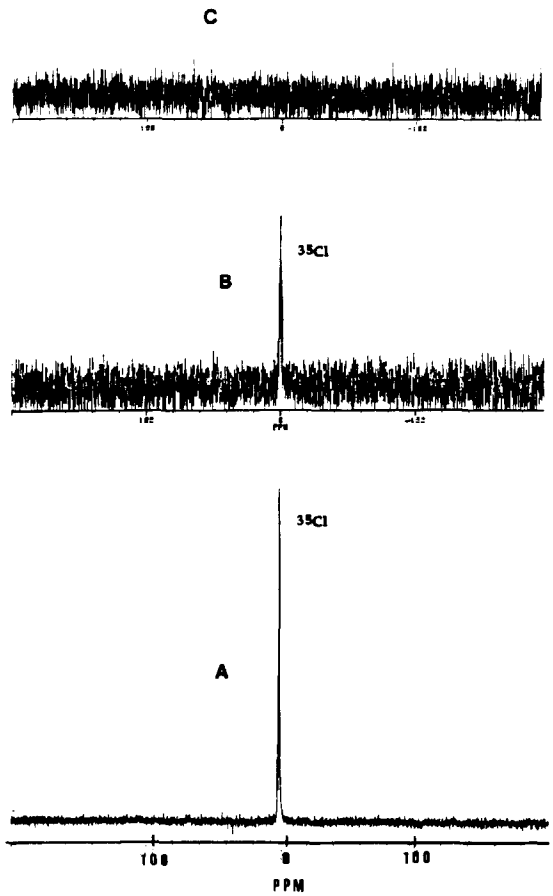

Fig. 8. ^{35}Cl-NMR spectra of (A) reference 10 mM Tris–HCl solution; (B) DDAB films after overnight soaking in 0.5 mM Mb in 10 mM TRIS + 50 mM NaCl, pH 7.5 and washing with water, and dispersing in ethanol; (C) DDAB films after overnight soaking in 10 mM TRIS + 50 mM NaCl, pH 7.5, not containing Mb, washing with water, and dispersing in ethanol ($^{35}Cl^-$ at 0 ppm).

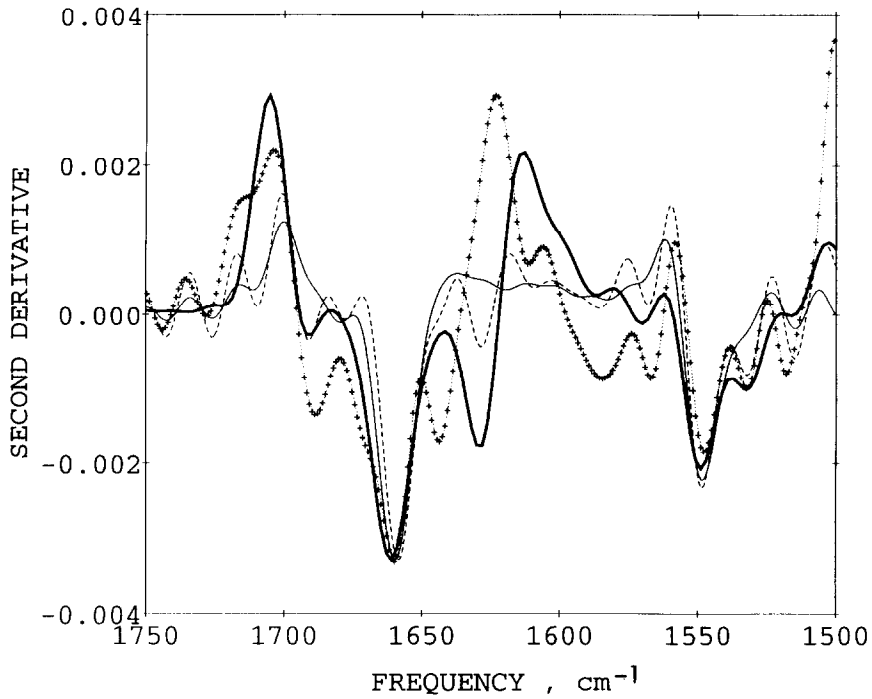

Fig. 9. Second derivative of absorbance from RAIR spectra at source incidence angle 60° for (————, thin) Mb film with no DDAB prepared using pH 5.5 buffer, and Mb-DDAB films prepared using buffers of (- - -) pH 7.5 + 50 mM NaCl, (· · · + · · ·) pH 5.5 + 50 mM NaBr, and (————, thick) pH 4.0 + 50 mM NaBr.

spectra for Mb-DDAB films prepared with buffers at pH 7.5, 5.5, and 4 is the strong α-helix band at 1660 cm^{-1} (Fig. 9). As film thickness is somewhat variable, it is best to compare ratios of the other bands in the spectra to this 1660 cm^{-1} band, which all have about the same intensity in Fig. 9. A small 1630 cm^{-1} band for the Mb-DDAB film is seen at pH 7.5, suggesting a very small increase in disorder compared to native Mb. At pH 5.5, this band is absent, but new, slightly larger bands appear at about 1646 and 1683 cm^{-1}, and are attributed to disordered loops and turns [40–42], respectively. These bands are not as large as the 1630 cm^{-1} band observed at pH 4. We conclude that at pH 4, several helices of Mb are beginning to unfold. At pH 5.5, the protein is slightly less unfolded, while at pH 7.5 the secondary structure is most like the native protein.

3.4. Model for the influence of pH

Models based on linked equilibria were tested for the pH dependencies and electrochemical parameters of Mb in the DDAB films. Expressions of the form of $Y_{obs} = F(Y_k, [H^+], K_j)$ were based on the overall equilibrium approach [43]. The K_j are proton association constants and the Y_k are parameters characteristic of contributions of individual forms of the protein. The model which best fit all the data is:

$$\mathrm{MbFe(III)\text{-}H_2O} + m\mathrm{H^+} \rightleftharpoons \mathrm{H}_m\mathrm{MbFe(III)} \quad -\mathrm{H_2O} \quad K_1 \qquad (1)$$

$$\mathrm{MbFe(III)\text{-}OH} + \mathrm{H^+} \rightleftharpoons \mathrm{MbFe(III)\text{-}H_2O} \quad K_2 \qquad (2)$$

where charges on Mb species are omitted. Eq. (1) represents the multiple protonations of Mb as it is titrated with acid [37,38,44–53]. Eq. (2) depicts the dissociation of the axial heme water of Mb at higher pH [44–46].

Eq. (3) was derived from thermodynamic linkage of the equilibria in Eqs. (1) and (2) by previously described methods [43]. It was used to fit data on

Table 2
Equilibrium constants[a] for Mb in DDAB films and in solution

Sample	Measured quantity	pK_{a1}	pK_{a2}	Ref.
Mb-DDAB films	$k^{0'}$ (cm s^{-1})	4.6 ± 0.1	7.4 ± 0.9	tw
	% Electroactive Mb	4.6 ± 0.9	8.3 ± 0.5	tw
	$E^{0'}$	4.8 ± 0.2	8.0 ± 0.3	tw
	Soret band Absorbance	4.2 ± 0.8	8.4 ± 0.7	[34]
Mb soln., I = 55 mM[b]	Soret band Absorbance	4.1 ± 0.5	8.3 ± 0.5	[34]
Mb soln., I = 105 mM[b]	Soret band Absorbance	4.4 ± 0.2	8.8 ± 0.2	[34]

[a] Expressed as acid dissociation constants, see text. pK_a given with standard errors from the regression analyses.
[b] I = ionic strength.

electron transfer rate constants and percent electroactive protein vs. pH:

$$Y_{obs} = \frac{Y_0}{1 + K_1^m[H^+]^m} + \frac{Y_1 K_1^m[H^+]^m}{1 + K_1^m[H^+]^m} + \frac{(Y_2 - Y_1)K_2[H^+]}{1 + K_2[H^+]} \quad (3)$$

where Y_{obs} is the measured quantity, and the Y_k are parameters characteristic of that measured quantity for the different forms of Mb. For example, when fitting $k^{0'}$ vs pH data with Eq. (3), Y_0 is the $k^{0'}$ for MbFe(III)–H_2O, Y_1 is $k^{0'}$ for H_mMbFe(III)–H_2O, and Y_3 is $k^{0'}$ for MbFe(III)–OH. Eq. (3) was fit to Y_{obs} vs. pH data by nonlinear regression using Y_0, Y_1, Y_2, K_1, and K_2 as parameters (Table 2). Best fits were found for $m = 1$. Goodness of fit is illustrated in Figs. 3 and 4.

Association constants found by regression analyses were converted to acid dissociation constants by using $pK_{aj} = -pK_j$ (Table 2). Values of pK_{a1} and pK_{a2} were also obtained [36] from intersection points in the $E^{0'}$ vs. pH plot (Fig. 2).

pK_{a1} values obtained from electrochemical data are self-consistent and similar to those from Soret band absorbance of Mb-DDAB films and Mb in solution. pK_{a2} values from the electrochemical data are slightly smaller than those found in solution.

4. Discussion

4.1. Dependence of voltammetry on pH

Previous studies by ESR, absorption spectroscopy, and linear dichroism showed [17,21] that high spin metmyoglobin [MbFe(III)–H_2O] predominates in Mb-DDAB films prepared with buffers of pH between 5.5 and 7.5. Metmyoglobin has a proximal histidine bound to iron below the plane of the heme, and a distal histidine hydrogen-bonded to ligated water above the heme [38,52,53].

Reversible changes in voltammograms with changes in pH and salt concentration of the external solution show that the properties of Mb within DDAB films can be controlled by the acidity and salt content of the solution in which the films reside. The model in Eq. (3) provided a good fit (Table 2 and Figs. 2–4) for the full pH dependencies of electrochemical parameters of these relatively thick Mb-DDAB films. Experiments summarized in Table 2 monitor properties of the Fe(III)heme of the protein, and are thus sensitive to structural changes involving the heme and its vicinity.

Similarities of pK_{a1} and pK_{a2} values in DDAB films to those of Mb in solution (Table 2) [38,44–46] suggest that similar effects on iron heme ligation and on secondary structure of Mb are operative in the films and in solutions. NMR studies [38,52,53] provided pK_a values for individual amino acid side chains of horse myoglobin in solution. The distal, proximal and four other histidines of Mb have pK_a-values between pH 4.3 and 5 [52]. The bond between proximal histidine and MbFe(III) may be broken below pH 5 [48,52]. These histidines may be associated with the pK_{a1} for Mb estimated in the films.

FT–IR spectra (Fig. 9) suggest partial unfolding of Mb in DDAB films at low pH. Between pH 5.5 and 7.5, Mb structure is similar to the native state conformation with about 75% helix [41,42]. Unfolding involving loss of helices is found for Mb at pH 4

in surfactant-free films [34]. In Mb-DDAB films at pH 4 the second derivative peak at 1630 cm^{-1} indicates significant unfolding (Fig. 9). Intensity of the α-helix band at 1659 cm^{-1} is lost at the expense of the 1630–1631 cm^{-1} band assigned to extended polypeptide chain. Integrations of the relevant peaks show that about 20% helix is lost in going from pH 7.5 to 4. The conformational transition occurs at pH values in the vicinity of pK_{a1}.

Dissociation of water bound to the Fe(III)heme of Mb (Eq. (2)) is responsible for pK_{a2} (Table 2). High spin metmyoglobin is converted to low spin MbFe(III)–OH [44–46]. Average pK_{a2} values were 8.0 for Mb-DDAB films. A slightly smaller pK_{a2} for Mb-DDAB than in solution (Table 2) may reflect the ability of DDAB, like other cationic surfactants [54] to preferentially attract OH^- to the vicinity of cationic head groups. This would make the pH in head group regions of the films higher than the pH of the external solution, shifting the apparent pK_{a2} to a smaller value. A similar effect was found in DDAB microemulsions, in which pH increased near DDAB head groups at water–oil interfaces [55].

4.2. Reduction pathways of Mb

Electrochemical results for Mb in DDAB films depended on pH in ways similar to, but not exactly the same as, thin films of dialkylphosphatidylcholines and DDAB [34]. Results of analyses of $E^{0'}$, percent electroactive Mb, and $k^{0'}$ vs. pH (Figs. 2–4) lead to the conclusion that reduction of Mb between pH 5 and 8 in DDAB films involves the transfer of one electron and one proton.

As pH decreases below 5, the fraction of electroactive protein (Fig. 3) and electron transfer rate constants begin to increase (Fig. 4), while the reduction potential shifts positive (Fig. 2). These changes in electrochemical parameters at $pH < 5$ are correlated with significant conformational changes in the protein found by spectroscopy. FT–IR spectra (Fig. 9) suggest that several helices of Mb are unraveled at low pH in DDAB films. These correlations, in conjunction with the pH dependence of $E^{0'}$, suggest that protonation of Mb precedes electron transfer. While protonation following electron transfer might be a possibility, it can not explain the increase in the fraction of electroactive Mb at $pH < pK_{a1}$. Such data were obtained by integration of the charge passed through the electrochemical cell during reduction of MbFe(III), and would not be influenced by a chemical event that occurs after this reduction [56].

Data between pH 5–8 are consistent with a mechanism proposed recently for reduction of Mb in thin surfactant films [34]. This involves protonation of metmyoglobin as in Eq. (1) prior to the electron transfer event (Eq. (4)). The protonations induce conformational change, leading to partial unfolding of MbFe(II) relative to native metmyoglobin, as reflected in FT–IR spectra in solution [57]. It is also possible that water dissociates from the Fe(II) after electron transfer, as reported previously for Mb in solution [18], but this reaction was not detected by voltammetry in Mb-DDAB films. Comparison of our pK_{a1} values (Table 2) with pK_a's of Mb side chains from NMR [52,53] suggests that protonation of the distal histidine and/or the proximal histidine originally bound to iron may control the pH dependence of the formal potential.

$$H_mMbFe(III)–H_2O + e^- \rightleftharpoons H_mMbFe(II)–H_2O \quad (4)$$

Spectroscopic studies of myoglobin and apomyoglobin in solution have identified a stable, salt-dependent, partly unfolded intermediate at $pH < 5$ known as a molten globule. Although much of this work has focused on apomyoglobin, myoglobin has a similar structure [37,38,50–53]. Compared to metmyoglobin, the molten globule intermediate has unfolded B, C, D, and E helices [38], involving about 30% loss of helix. At $pH < 5$, spectroscopic results (Fig. 9) show that a partly unfolded MbFe(III) begins to predominate in the films. Combined with the pH-independence of $E^{0'}$ at $pH < 4.8$, this suggests that a molten globule-like Mb is reduced directly in this low range of external pH. On the other hand, it is unlikely that the equilibrium molten globule is the electron acceptor at pH 5–8, since the time needed for unfolding is probably much longer than the voltammetric time scale [34].

The nearly pH-independent region in the $E^{0'}$ vs. pH plot (Fig. 2) for Mb-DDAB at $pH > 8$ suggests direct reduction of the low spin MbFe(III)–OH form. This is also consistent with the increase in $k^{0'}$ at $pH > 7$, since low spin MbFe(III) is reduced more rapidly than high spin metmyoglobin [18].

4.3. Influence of salt

NMR spectra (Fig. 8) suggest that anions are strongly associated with Mb within the films. These experiments complement previous bromide analyses of films by EDX [17], which showed that Br^- was lost from DDAB films only in solutions containing acetate or Cl^- and Mb. Bound anions, or more generally bound salt, may neutralize the surface charge of Mb, facilitating partial insertion of the protein into surfactant bilayers in the films. Partly hydrophobic residence sites for Mb in DDAB films were suggested by linear dichroism and ESR studies [24].

The fraction of molten globule apomyoglobin in solution increases with increasing salt concentration [37,50]. Also, interfacial Donnan potentials may contribute to formal potentials of electroactive ions in polyion films [58]. Thus, the concentration of salt in solution may influence the electrochemistry of Mb in the films by changing protein conformation and/or by influencing the interfacial Donnan potential of the film.

Under ideal conditions where the amount of salt within the film does not change with the salt concentration in solution, Donnan potentials should cause $E^{0'}$ of Mb to shift by 59 mV/log[S] at 25°C, where [S] is the external salt concentration [58]. Data in Table 1 agree qualitatively with this prediction, with S = NaBr results at pH 4 and 7.5 giving slopes closest to the theoretical prediction. Thus, Donnan potentials may be controlling factors in the salt dependence of $E^{0'}$.

There were small but significant increases in electron transfer rate constants (Fig. 7) with increasing salt concentration in every film examined. This effect is smallest at pH 4 (Table 1). The increase in $k^{0'}$ may be related to penetration of salt into the films, which contain 40–60% water [24]. Salt-induced facilitation of Mb unfolding may make the iron heme group more accessible to the electrode and increase the apparent heterogeneous electron transfer rate constants.

At pH 4, there is a strong salt dependence of percent electroactive Mb in the DDAB films, with a maximum at about 50 mM NaBr (Fig. 5). A similar but smaller maximum in percent electroactive Mb occurs at about 70 mM NaBr at pH 5.5, but no maximum is seen at pH 7.5. This is again consistent with salt-dependent unfolding, since pH 4–5.5 is near the native-to-molten globule transition region in the apomyoglobin unfolding phase diagram [37]. In this region of pH, the ratio of molten globule-to-native Mb is very sensitive to salt concentration, but at pH 7.5 the molten globule cannot be formed.

5. Summary

The pH and salt concentration of external solutions control the electrochemical properties of Mb in thick DDAB films. In solutions of pH between 5 and 8, protonation preceding electron transfer from electrodes to aquometmyoglobin (MbFe(III)–H_2O) controls $E^{0'}$. This is similar to behavior found in thin dialkylphosphatidycholine (PC) or DDAB films [34]. At pH > 8 in Mb-DDAB films, MbFe(III)–H_2O dissociates to MbFe(III)–OH, which is reduced directly at the electrode. At pH < 4.6, a partly unfolded form of Mb is reduced in DDAB films. $E^{0'}$ is nearly independent of pH in both of these pH ranges.

Salt may play an integral role in governing electrochemical properties and stability of the films. NMR spectra suggest strong binding of anions to Mb within the films. These bound anions may neutralize surface charge so that the protein can reside in a partly hydrophobic environment, as postulated on the basis of previous ESR and linear dichroism studies [24]. Furthermore, salt concentration in solution has a significant influence on electrochemical properties of the Mb-DDAB films through the Donnan effect and through its influence on Mb conformation.

Acknowledgements

This work was supported by US PHS grant No. ES03154 from NIH awarded by the National Institute of Environmental Health Sciences. Its contents are solely the responsibility of the authors and do not necessarily represent the official views of NIEHS, NIH. The authors thank Dr. Thomas Leipert of Univ. of Connecticut for assistance with NMR.

References

[1] F.A. Armstrong, H.A.O. Hill, N.J. Walton, Acc. Chem. Res. 21 (1988) 407.
[2] F.A. Armstrong, Bioinorg. Chem. Struct. Bonding 72 (1990) 137.
[3] A. Heller, Acc. Chem. Res. 23 (1990) 128.
[4] M.J. Tarlov, E.F. Bowden, J. Am. Chem. Soc. 113 (1991) 1847.
[5] S. Song, R.A. Clark, E.F. Bowden, M.J. Tarlov, J. Phys. Chem. 97 (1993) 6564.
[6] J.H. Reeves, S. Song, E.F. Bowden, Anal. Chem. 65 (1993) 683.
[7] T.M. Nahir, R.A. Clark, E.F. Bowden, Anal. Chem. 66 (1994) 2595.
[8] M. Collinson, E.F. Bowden, Langmuir 8 (1992) 1247.
[9] S.M. Amador, J.M. Pachence, R. Fischetti, J.P. McCauley, A.B. Smith, J.K. Blasie, Langmuir 9 (1993) 2255.
[10] K.T. Kinnear, H.G. Monbouquette, Langmuir 9 (1993) 2255.
[11] Z. Salamon, G. Tollin, Bioelectrochem. Bioenerg. 25 (1991) 447.
[12] Z. Salamon, G. Tollin, Bioelectrochem. Bioenerg. 27 (1992) 381.
[13] Z. Salamon, F.K. Gleason, G. Tollin, Arch. Biochem. Biophys. 299 (1992) 193.
[14] H.T. Tien, Z. Salamon, Bioelectrochem. Bioenerg. 22 (1989) 211.
[15] M. Snejdarkova, M. Rehak, M. Otto, Anal. Chem. 65 (1993) 665.
[16] J.K. Cullison, F.M. Hawkridge, N. Nakashima, C.R. Hartzell, in: M.J. Allen et al. (Eds.), Charge and Field Effects in Biosystems-3, Birkhauser, Boston, 1992, pp. 29–39.
[17] J.F. Rusling, A.-E.F. Nassar, J. Am. Chem. Soc. 115 (1993) 11891.
[18] B.C. King, F.M. Hawkridge, B.M. Hoffman, J. Am. Chem. Soc. 114 (1992) 10603.
[19] I. Taniguchi, K. Watanabe, M. Tominaga, F.M. Hawkridge, J. Electroanal. Chem. 333 (1992) 331.
[20] I. Taniguchi, H. Kurihara, K. Yoshida, M. Tominaga, F.M. Hawkridge, Denki Kagaku 60 (1992) 1043.
[21] A.-E.F. Nassar, Y. Narikiyo, T. Sagara, N. Nakashima, J.F. Rusling, J. Chem. Soc., Faraday Trans. 91 (1995) 1775.
[22] Z. Zhang, J.F. Rusling, Biophys. Chem. 63 (1997) 133.
[23] A.-E.F. Nassar, W.S. Willis, J.F. Rusling, Anal. Chem. 67 (1995) 2386.
[24] A.-E.F. Nassar, Z. Zhang, V. Chynwat, H.A. Frank, J.F. Rusling, K. Suga, J. Phys. Chem. 99 (1995) 110.
[25] Z. Zhang, A.-E.F. Nassar, Z. Lu, J.B. Schenkman, J.F. Rusling, J. Chem. Soc., Faraday Trans. 93 (1997) 1769.
[26] Z. Lu, Q. Huang, J.F. Rusling, J. Electroanal. Chem. (1997) in press.
[27] P. Bianco, J. Haladjian, J. Electroanal. Chem. 367 (1994) 79.
[28] P. Bianco, J. Haladjian, Electrochim. Acta 39 (1994) 911.
[29] J. Hanzlik, P. Bianco, J. Haladjian, J. Electroanal. Chem. 380 (1995) 287.
[30] P. Bianco, J. Haladjian, Electroanalysis 7 (1995) 442.
[31] M. Tominaga, J. Yanagimoto, A.-E.F. Nassar, J.F. Rusling, N. Nakashima, Chem. Lett. (1996) 523.
[32] A.-E.F. Nassar, J.F. Rusling, M. Tominaga, J. Yanagimotoa, N. Nakashima, J. Electroanal. Chem. 416 (1996) 183.
[33] A.-E.F. Nassar, J.M. Bobbitt, J.D. Stuart, J.F. Rusling, J. Am. Chem. Soc. 117 (1995) 10986.
[34] A.-E.F. Nassar, Z. Zhang, J.F. Rusling, T.F. Kumosinski, J. Phys. Chem. 101 (1997) 2224.
[35] J. Heyrovsky, J. Kuta, Principles of Polarography, Academic Press, New York, 1966.
[36] A.M. Bond, Modern Polarographic Methods in Analytical Chemistry, Marcel Dekker, New York, 1980, pp. 29–30.
[37] Y. Goto, A.L. Fink, J. Mol. Biol. 214 (1990) 803.
[38] A.-S. Yang, B. Honig, J. Mol. Biol. 237 (1994) 602.
[39] H. Susi, D.M. Byler, Meth. Enzymol. 130 (1986) 290.
[40] A. Dong, P. Huang, W.S. Caughey, Biochemistry 29 (1990) 3303.
[41] T.F. Kumosinski, J.J. Unruh, Talanta 43 (1996) 199.
[42] J.F. Rusling, T.F. Kumosinski, Nonlinear Computer Modeling of Chemical and Biochemical Data, Academic Press, New York, 1996, pp. 117–134.
[43] J.F. Rusling, T.F. Kumosinski, Nonlinear Computer Modeling of Chemical and Biochemical Data, Academic Press, New York, 1996, pp. 87–116.
[44] H. Theorell, A. Ehrenberg, Acta Chem. Scand. 5 (1951) 823.
[45] P. George, G. Hanania, Biochem. J. 52 (1952) 517.
[46] M. Brunori, G.M. Giacometti, E. Antonini, J. Wyman, J. Mol. Biol. 63 (1972) 139.
[47] E. Takahashi-Ushijima, H. Kihara, Biochem. Biophys. Res. Comm. 105 (1982) 965.
[48] D. Puett, J. Biol. Chem. 248 (1973) 4623.
[49] H.-L. Tang, B. Chance, A.G. Mauk, L.S. Powers, K.S. Reddy, M. Smith, Biochem. Biophys. Acta 1206 (1994) 90.
[50] D. Stigter, D.O.V. Alonso, K.A. Dill, Proc. Natl. Acad. Sci. USA 88 (1991) 4176.
[51] S.H. Friend, F.R.N. Gurd, Biochemistry 18 (1979) 4612.
[52] D. Bashford, D.A. Case, C. Dalvit, L. Tennant, P.E. Wright, Biochemistry 32 (1993) 8045.
[53] M.J. Cocco, Y.-H. Kao, A.T. Phillips, J.T.J. Lecomte, Biochemistry 31 (1992) 6481.
[54] J.H. Fendler, E.J. Fendler, Catalysis in Micellar and Macromolecular Systems, Academic Press, New York, 1975.
[55] G. Gounili, C.L. Miaw, J.M. Bobbitt, J.F. Rusling, J. Colloid Interface Sci. 153 (1992) 446.
[56] A.J. Bard, L.R. Faulkner, Electrochemical Methods, Wiley, New York, 1980, pp. 429–483.
[57] D.D. Schlereth, W. Mantele, Biochemistry 31 (1992) 7494.
[58] R. Naegeli, J. Redpenning, F.C. Anson, J. Phys. Chem. 90 (1986) 6227.